

# Highly Luminescent $(\text{Zn}_{0.6}\text{Sr}_{0.3}\text{Mg}_{0.1})_2\text{Ga}_2\text{S}_5:\text{Eu}^{2+}$ Green Phosphors for a White Light-Emitting Diode

Yong-Kwang Jeong, Dong-Hee Cho, Kwang-Bok Kim,<sup>†</sup> and Jun-Gill Kang<sup>\*</sup>

Department of Chemistry, Chungnam National University, Daejeon 305-764, Korea. \*E-mail: jgkang@cnu.ac.kr

<sup>†</sup>Kumho Electric Inc., Youngin, Gyeonggi-Do 449-883, Korea

Received September 9, 2011, Accepted May 1, 2012

Green phosphors  $(\text{Zn}_{1-a-b}\text{M}_a\text{M}'_b)_x\text{Ga}_y\text{S}_{x+3y/2}:\text{Eu}^{2+}$  ( $\text{M}, \text{M}' =$  alkali earth ions) with  $x = 2$  and  $y = 2-5$  were prepared, starting from  $\text{ZnO}$ ,  $\text{MgO}$ ,  $\text{SrCO}_3$ ,  $\text{Ga}_2\text{O}_3$ ,  $\text{Eu}_2\text{O}_3$ , and  $\text{S}$  with a flux  $\text{NH}_4\text{F}$  using a conventional solid-state reaction. A phosphor with the composition of  $(\text{Zn}_{0.6}\text{Sr}_{0.3}\text{Mg}_{0.1})_2\text{Ga}_2\text{S}_5:\text{Eu}^{2+}$  produced the strongest luminescence at a 460-nm excitation. The observed XRD patterns indicated that the optimized phosphor consisted of two components: zinc thiogallate and zinc sulfide. The characteristic green luminescence of the  $\text{ZnS}:\text{Eu}^{2+}$  component on excitation at 460 nm was attributed to the donor-acceptor ( $\text{D}_{\text{ZnGa}_2\text{S}_4}-\text{A}_{\text{ZnS}}$ ) recombination in the hybrid boundary. The optimized green phosphor converted 17.9% of the absorbed blue light into luminescence. For the fabrication of light-emitting diode (LED), the optimized phosphor was coated with  $\text{MgO}$  using magnesium nitrate to overcome their weakness against moisture. The  $\text{MgO}$ -coated green phosphor was fabricated with a blue  $\text{GaN}$  LED, and the chromaticity index of the phosphor-cast LED (pc-LED) was investigated as a function of the wt % of the optimized phosphor. White LEDs were fabricated by pasting the optimized green (G) and the red (R) phosphors, and the commercial yellow (Y) phosphor on the blue chips. The three-band pc-WLED resulted in improved color rendering index (CRI) and corrected color temperature (CCT), compared with those of the two-band pc-WLED.

**Key Words :** Two-component green luminescence, Donor-Acceptor recombination,  $\text{MgO}$  coating, White LED

## Introduction

Currently, white LEDs have been commercially produced through the combination of a blue LED and a yellow modified-YAG: $\text{Ce}^{3+}$  ( $(\text{Y}_{1-a}\text{Gd}_a)_3(\text{Al}_{1-b}\text{Ga}_b)_5\text{O}_{12}:\text{Ce}^{3+}$ ) phosphor. The luminescence efficiency of the two-color white LED increases steadily and fabrication costs are low. The color properties of conventional two-band white LEDs, however, do not fully meet the requirements for general lighting applications because of their low color rendering. Multiple color phosphors with strong green, yellow and red luminescence are necessary for highly efficient full-color white LEDs. Alkali earth thiogallate phosphors doped with  $\text{Eu}^{2+}$  have attracted much interest for applications in white LED and electroluminescence and cathodoluminescence devices because they exhibit strong green or yellow luminescence, depending on the alkali earth ion. Phosphors of  $\text{MGa}_2\text{S}_4:\text{Eu}^{2+}$  ( $\text{M} = \text{Sr}$  and  $\text{Zn}$ ) excited with blue light produce green luminescence peaking at 540 nm.<sup>1-6</sup> Nazarov *et al.* synthesized an  $\text{Eu}^{2+}$ -doped multiphase green phosphor composed of  $\text{SrGa}_2\text{S}_4$  and  $\text{MgGa}_2\text{O}_4$ .<sup>7</sup> It was found that the multiphase phosphor exhibited higher intensity and a better chromaticity coordinate than a known commercial  $\text{SrGa}_2\text{S}_4:\text{Eu}^{2+}$  phosphor. These optical properties of the multiphase phosphor make it a very attractive candidate for white LEDs.

In this study, we prepared alkali earth ion-substituted zinc-gallium-sulfide phosphors doped with  $\text{Eu}^{2+}$ ,  $(\text{Zn}_{1-a-b}\text{M}_a\text{M}'_b)_x\text{Ga}_y\text{S}_{x+3y/2}:\text{Eu}^{2+}$  ( $\text{M}, \text{M}' =$  alkali earth ions), using a solid-

state reaction, and investigated the effects of alkali earth ions on the luminescence properties. We optimized the phosphor by measuring the relative intensity and the quantum yield as a function of the concentration of the alkali earth,  $\text{Ga}^{3+}$  and  $\text{Eu}^{2+}$  ions. Additionally, we coated a thin  $\text{MgO}$  layer on the synthesized green phosphor to reduce the surface degradation of sulfide phosphors associated with device fabrication processes and improve dispersion and adhesion properties.<sup>8,9</sup> Subsequently, we packed the  $\text{MgO}$ -coated phosphor on a  $\text{GaN}$  chip and characterized the emitted light.

## Experimental

**Synthesis.** Typically, host materials of the sulfides have been prepared by reaction of the oxides or carbonates using  $\text{H}_2\text{S}$  gas. However, this method is toxic and costly. In this work, the sulfide phosphors were prepared using a solid-state reaction with sulfur. The starting materials (purity > 99.9%),  $\text{ZnO}$ ,  $\text{MgO}$ ,  $\text{SrCO}_3$ ,  $\text{Ga}_2\text{O}_3$ ,  $\text{Eu}_2\text{O}_3$ , and  $\text{S}$  were purchased from Aldrich. They were taken in stoichiometric proportions, with  $\text{S}$  in excess. A mixture was prepared by thoroughly grinding the materials mixed with a few wt % of  $\text{NH}_4\text{F}$  as a flux in an agate mortar and transferring the mixture to a capped alumina crucible. The mixture was fired at 850 °C for 2 h under a  $\text{N}_2/\text{H}_2$  reducing atmosphere in a tube furnace. After the first firing, the samples were reground and fired again at 950 °C under the same condition.

**Characterization.** The X-ray diffraction (XRD) patterns

of the prepared phosphor were measured using a D/MAX-2200 Ultima diffractometer (Rigaku) with a graphite monochromator and Cu K $\alpha$  radiation ( $\lambda = 0.1541$  nm). The luminescence and excitation spectra were measured with an ARC 0.5-m Czerny-Turner monochromator (equipped with a cooled Hamamatsu R-933-14 PM tube). The excitation light was from a 1000-W Xe lamp (working power, 400 W; Oriol) passing through an Oriol MS257 monochromator. The luminescence quantum yield, defined by

$$Q = \frac{\text{number of photons emitted}}{\text{number of photons absorbed}}$$

was determined using a previously described method.<sup>10</sup> The recorded spectra for the quantum yield were corrected for the spectral response of the system using an Oriol 45-W quartz tungsten halogen lamp standard. All measurements were repeated three times. No significant experimental error was found.

The surface of the synthesized phosphor was coated with MgO using a standard sol-gel process with magnesium nitrate (Aldrich) as a precursor. The phosphor (12 g) was added to the precursor solution (500 mL). Here, the concentration of the precursor was fixed at 10 wt %. The pH of the resulting solution was adjusted to 11 using ammonia water. After stirring for 3 h, the coated phosphor was filtered and fired in air at 400 °C for 2 h. Morphologies of uncoated and MgO-coated phosphors were determined by field emission scanning electron microscopy (FE-SEM) and energy dispersive (ED) spectroscopy. SEM micrographs and ED spectra were acquired with a JSM-7000F FE-SEM (JEOL, Tokyo, Japan).

For the phosphor-casted LED (pc-LED) fabrication, the MgO-coated phosphors, sieved under  $\phi = 20$   $\mu\text{m}$ , were mixed with epoxy at various wt %s and cast on the lead frame of a blue GaN LED chip. The pc-LED was dried at 80 °C for 12 h under a vacuum condition. To measure the optical properties, the pc-LEDs were installed in an integrating sphere, and the luminescence spectra were recorded with a Spectra pro 2300i (Acton). The spectral data were evaluated with a Darsa MONO XP (v. 5.0).

## Results and Discussion

**Phase and Morphology.** XRD data were collected for the optimized  $\text{Zn}_2\text{Ga}_2\text{S}_5:\text{Eu}^{2+}$  and  $(\text{Zn}_{0.6}\text{Sr}_{0.3}\text{Mg}_{0.1})_2\text{Ga}_2\text{S}_5:\text{Eu}^{2+}$  and the peak positions of XRD patterns were analyzed with a reported ICSD database. As shown in Figure 1, all observed peaks of  $\text{Zn}_2\text{Ga}_2\text{S}_5:\text{Eu}^{2+}$  were in good agreement with a combination of ZnS (ICSD #15742) and  $\text{ZnGa}_2\text{S}_4$  (ICSD #635305). For Sr-substituted  $(\text{Zr}_{0.6}\text{Sr}_{0.3}\text{Mg}_{0.1})_2\text{Ga}_2\text{S}_5:\text{Eu}^{2+}$ , the intensities of three peaks at  $2\theta = 16.84$ ,  $23.96$  and  $38.36^\circ$  (indicated by \*) significantly increased, compared with the cases of  $\text{Zn}_2\text{Ga}_2\text{S}_5:\text{Eu}^{2+}$ . The intensities of these three peaks would be reinforced by  $\text{SrGa}_2\text{S}_4$ , because they are coincided with the main peaks of  $\text{SrGa}_2\text{S}_4$ . It was assumed that the optimized  $(\text{Zn}_{0.6}\text{Sr}_{0.3}\text{Mg}_{0.1})_2\text{Ga}_2\text{S}_5:\text{Eu}^{2+}$  green phosphor might consist of zinc thiogallate and zinc

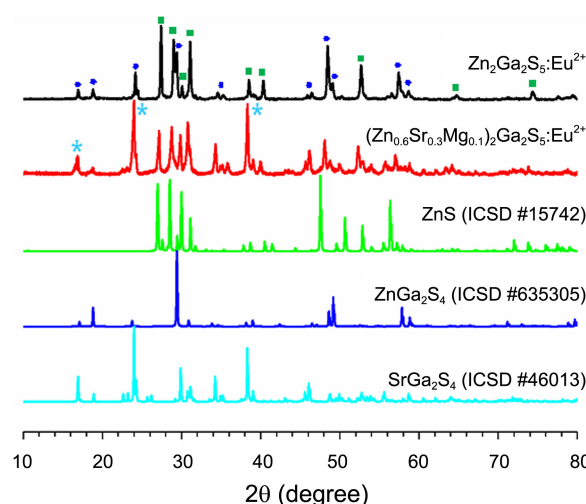


**Figure 1.** XRD patterns of  $\text{Zn}_2\text{Ga}_2\text{S}_5:\text{Eu}^{2+}$  and  $(\text{Zn}_{0.6}\text{Sr}_{0.3}\text{Mg}_{0.1})_2\text{Ga}_2\text{S}_5:\text{Eu}^{2+}$  phosphors, compared with reference ZnS (■),  $\text{ZnGa}_2\text{S}_4$  (●) and  $\text{SrGa}_2\text{S}_4$  (▲).

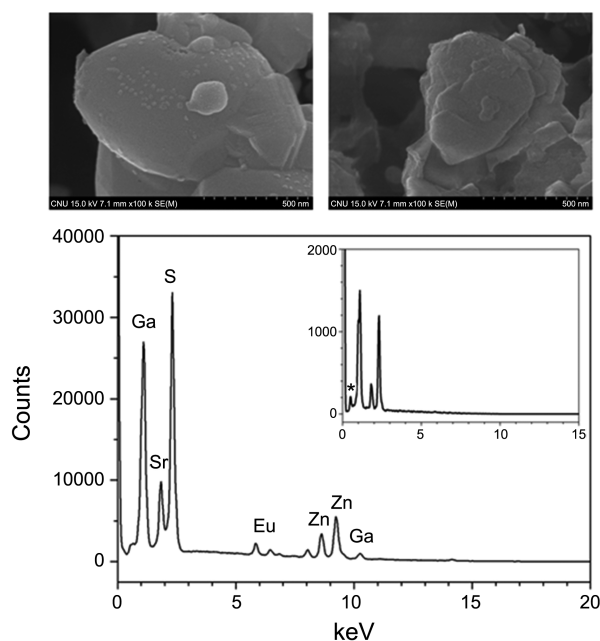


**Figure 2.** FE-SEM images of uncoated (upper left) and MgO-coated (upper right) green phosphors treated with 10 wt % of magnesium nitrate, and ED spectrum (lower) of uncoated phosphor (ED spectrum of MgO-coated phosphor inserted).

sulfide as a main components and strontium thiogallate as a minor component, where each divalent ion might be partially replaced by the other ions.

For the LED fabrication, the prepared green phosphor was coated with MgO by a sol-gel method. Figure 2 shows FE-SEM images and ED spectra of the uncoated and the MgO-coated phosphors. The surface of the uncoated green phosphor was smooth and clean, but some particles adhered to the uncoated green phosphors. Those particles were completely covered with MgO film when it was treated with 10% of the precursor. As seen in the inserted ED spectrum, O peak (indicated by \*) was observed at 0.5 keV for the

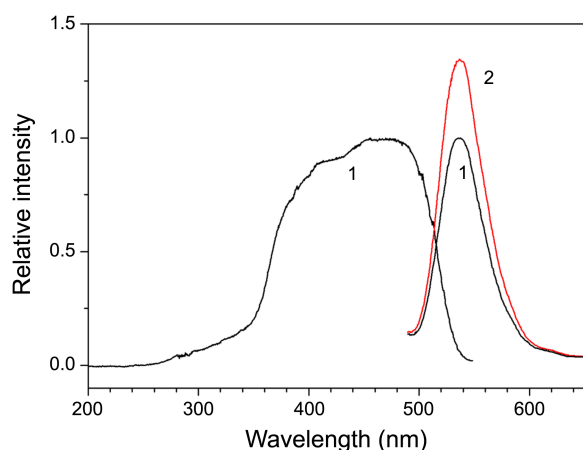


**Figure 3.** Emission ( $\lambda_{\text{exn}} = 460$  nm) spectra of  $\text{Zn}_2\text{Ga}_2\text{S}_5:\text{Eu}^{2+}$  (1) and  $\text{ZnGa}_2\text{S}_4:\text{Eu}^{2+}$  (2), and excitation ( $\lambda_{\text{ems}} = 560$  nm) spectrum of  $\text{Zn}_2\text{Ga}_2\text{S}_5:\text{Eu}^{2+}$  (1).

MgO-coated phosphor, while the intensities of Eu, Zn, Ga and Sr peaks in the high energy region were quenched due to the coated MgO film. These results indicated that the surface of the green phosphor well covered with MgO film.

**Luminescence Properties.** Figure 3 shows the emission spectra of  $\text{ZnGa}_2\text{S}_4:0.2\text{Eu}^{2+}$  and  $\text{Zn}_2\text{Ga}_2\text{S}_5:0.2\text{Eu}^{2+}$ , and the excitation spectrum of the green emission from  $\text{ZnGa}_2\text{S}_4:0.2\text{Eu}^{2+}$ . The 460-nm excitation produced green emissions from the two phosphors, peaking at 537 nm. Two characteristic features in the luminescence were noted:  $\text{Zn}_2\text{Ga}_2\text{S}_5:0.2\text{Eu}^{2+}$  was stronger than  $\text{ZnGa}_2\text{S}_4:0.2\text{Eu}^{2+}$ , and the optimum  $\text{Eu}^{2+}$  concentration in each phosphor was 0.16-0.24 moles with respect to the formula of each phosphor. Here, the  $\text{ZnS}:\text{Eu}^{2+}$  phosphor was observed to produce the blue or the green luminescence, depending on the particle size.<sup>11-14</sup> In nanocrystalline state, the green luminescence peaked at 530 nm upon excitation at 260 nm, and in bulk state, it peaked at 460 nm on excitation at 337 nm, as shown in Figure 4. The blue emission from  $\text{ZnS}:\text{Eu}^{2+}$  was very low: its intensity was much less than one tenth of the green emission from  $\text{ZnGa}_2\text{S}_4:\text{Eu}^{2+}$ . The color of the  $\text{ZnS}:\text{Eu}^{2+}$  phosphor was white and the 460-nm excitation did not produce a green emission from

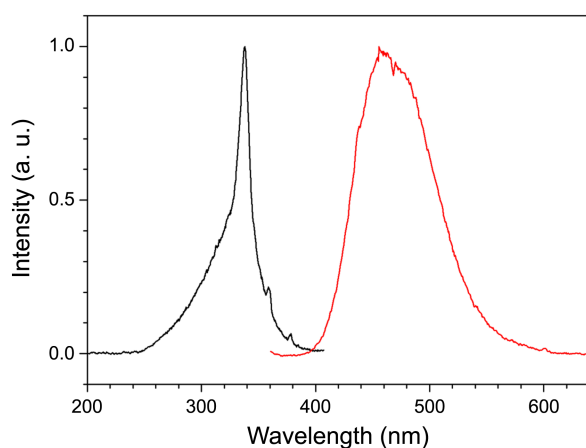


**Figure 4.** Emission ( $\lambda_{\text{exn}} = 337$  nm) and excitation ( $\lambda_{\text{ems}} = 460$  nm) spectra of  $\text{ZnS}:\text{Eu}^{2+}$ .

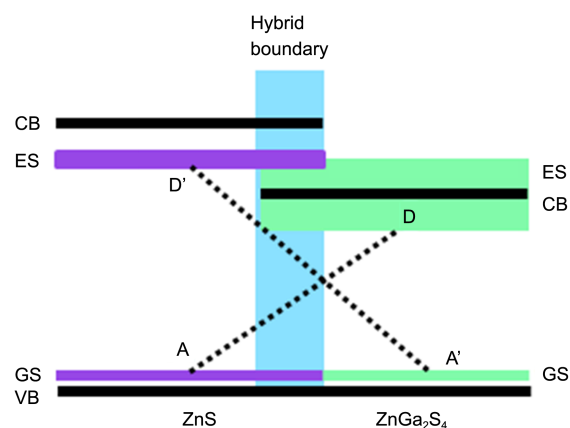


**Figure 5.** Schematic energy-level diagram of the hybrid  $\text{ZnS}:\text{Eu}^{2+}$ - $\text{ZnGa}_2\text{S}_4:\text{Eu}^{2+}$  boundary, representing the possible origin of the green emission from  $\text{ZnS}:\text{Eu}^{2+}$ .

$\text{ZnS}:\text{Eu}^{2+}$ . The excitation band of the blue emission from  $\text{ZnS}:\text{Eu}^{2+}$  was very narrow and the excited energy (3.68 eV) was slightly lower than the band-gap energy of the hexagonal  $\text{ZnS}$  (3.91 eV). The ground and the excited states of the  $\text{Eu}^{2+}$  defect lie close to the valence and the conduction bands of the host  $\text{ZnS}$ , respectively. The excitation band of the green emission from  $\text{ZnGa}_2\text{S}_4:\text{Eu}^{2+}$ , spanning over the 350-500 nm (2.48-3.54 eV) region, was very broad, as shown in Figure 3. Taking into account the band gap of  $\text{ZnGa}_2\text{S}_4$  (3.18 eV), the excited state of the  $\text{Eu}^{2+}$  defect might partially overlap with the conduction band of the  $\text{ZnGa}_2\text{S}_4$  host. The  $\text{Zn}_2\text{Ga}_2\text{S}_5:\text{Eu}^{2+}$  phosphor was very bright green, indicating that its phase was homogeneous. The two components of  $\text{ZnS}:\text{Eu}^{2+}$  and  $\text{ZnGa}_2\text{S}_4:\text{Eu}^{2+}$  in the  $\text{Zn}_2\text{Ga}_2\text{S}_5:\text{Eu}^{2+}$  phosphor would be coherent each other to form a hybrid boundary as shown in Figure 5. In the hybrid boundary, the electrostatic interaction between the two different  $\text{Eu}^{2+}$  defects resulted in an appropriate donor-acceptor pair recombination,  $\text{D}_{\text{ZnGa}_2\text{S}_4}-\text{A}_{\text{ZnS}}$  (D-A) and  $\text{D}_{\text{ZnS}}-\text{A}_{\text{ZnGa}_2\text{S}_4}$  (D'-A'). The donor and the acceptor ions were initially in the excited and the ground states, respectively, and the energy transfer took place from the donor to the acceptor. The D-A pair recombination can be responsible for the observed strong emission from the  $\text{ZnS}:\text{Eu}^{2+}$  component on excitation at 460 nm. Here, the  $\text{D}_{\text{ZnS}}-\text{A}_{\text{ZnGa}_2\text{S}_4}$  pair recombination was excluded, because the population rate of  $\text{D}_{\text{ZnS}}$  (D') was very low.

Taking into account these primary results, we investigated the  $\text{Sr}^{2+}$ -substitution effect on the luminescence of  $(\text{Zn}_{1-x}\text{Sr}_x)_2\text{Ga}_2\text{S}_5:0.2\text{Eu}^{2+}$ . As shown in Figure 6(a), an increased mole fraction of  $\text{Sr}^{2+}$  increased the luminescence intensity, and the peak position red-shifted slightly. When  $x = 0.4$ , the intensity reached a maximum. Above  $x = 0.4$ , the luminescence intensity decreased with increasing  $x$ . Additionally, we investigated the substitution effects of the other alkali earth ions. Surprisingly,  $\text{Ca}^{2+}$  and  $\text{Ba}^{2+}$  ions resulted in a reduction of the luminescence intensity. However, the partial replacement of  $\text{Sr}^{2+}$  with  $\text{Mg}^{2+}$  significantly affected the luminescence intensity, as shown in Figure 6(b). For the

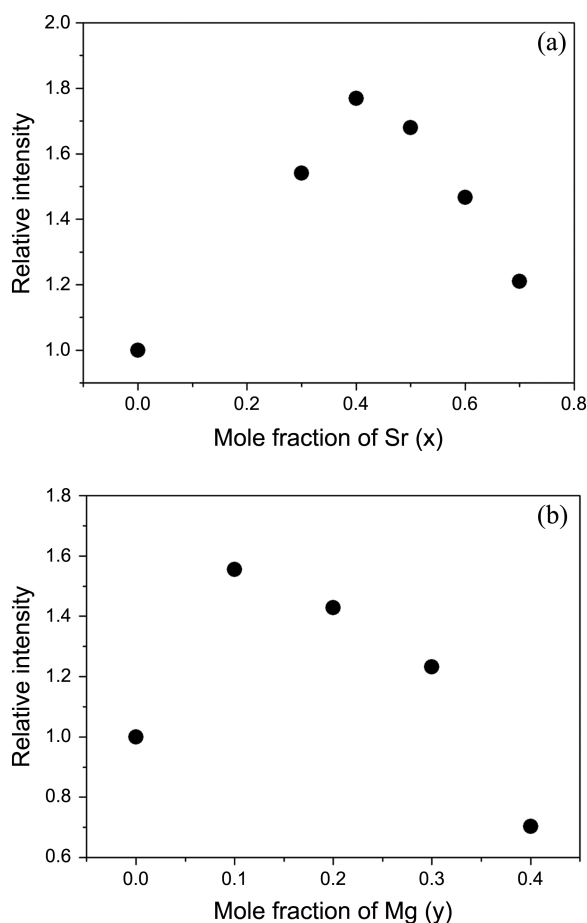


**Figure 6.** Relative intensities of  $(Zn_{1-x}Sr_x)_2Ga_2S_5:Eu^{2+}$  (a) and  $(Zn_{0.6}Sr_{0.4-y}Mg_y)_2Ga_2S_5:Eu^{2+}$  (b).

composition of  $(Zn_{0.6}Sr_{0.4-y}Mg_y)_2Ga_2S_5:0.2Eu^{2+}$ , an increased value of y increased the luminescence intensity, reaching a maximum at  $y = 0.1$ . Above  $y = 0.1$ , the intensity decreased with increasing y. Moreover, we also investigated the quantum yield of  $(Zn_{0.6}Sr_{0.3}Mg_{0.1})_2Ga_2S_5:0.2Eu^{2+}$  as a function of z. As shown in Figure 7, when  $z = 1$ , Q was 15.0%. With an increased value of z, the quantum yield increased and reached a maximum at  $z = 2$  ( $Q = 17.9\%$ ). Above  $z = 2$ , the quantum yield gradually decreased. Figure 8 shows the comparison between the luminescence spectra of the optimized  $(Zn_{0.6}Sr_{0.3}Mg_{0.1})_2Ga_2S_5:Eu^{2+}$ , two commercial green phosphors,  $CaBaSrSiO_4:Eu^{2+}$  (LWB) and  $\beta-SiAlON:Eu^{2+}$  (Denka), and modified  $YAG:Ce^{3+}$  (Nemoto-432). Recently, the green  $Ca_8Mg(SiO_4)_4Cl_2:Eu^{2+}, Mn^{2+}$  phosphor was prepared for a WLED.<sup>15</sup> The relative intensity (the bandwidth at half-maximum/nm) was 2.0 (45.5) for  $(Zn_{0.6}Sr_{0.3}Mg_{0.1})_2Ga_2S_5:Eu^{2+}$ , 1.3 (73.5) for  $CaBaSrSiO_4:Eu^{2+}$  (LWB), 1.4 (61.4) for  $\beta-SiAlON:Eu^{2+}$  (Denka), 1.5 (45.0) for  $Ca_8Mg(SiO_4)_4Cl_2:Eu^{2+}, Mn^{2+}$  and 1 (113.6) for modified  $YAG:Ce^{3+}$  (Nemoto-432). The optimized phosphor has stronger intensity and narrower bandwidth than the two commercial and silicate green phosphors. This result indicated that the colority of  $(Zn_{0.6}Sr_{0.3}Mg_{0.1})_2Ga_2S_5:Eu^{2+}$  is better than those of the two commercial green phosphors and  $Ca_8Mg(SiO_4)_4Cl_2:Eu^{2+}, Mn^{2+}$ . Although the luminescence intensity of the prepared

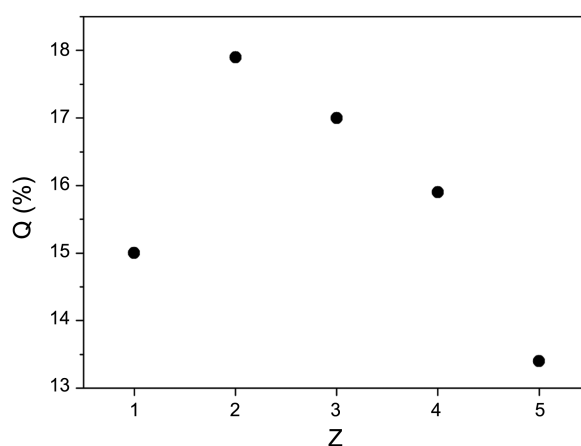


**Figure 7.** Quantum yields of  $(Zn_{0.6}Sr_{0.3}Mg_{0.1})_2Ga_zS_{2+3z/2}:0.20Eu^{2+}$  ( $1 \leq z \leq 5$ ,  $\lambda_{exn} = 460$  nm).

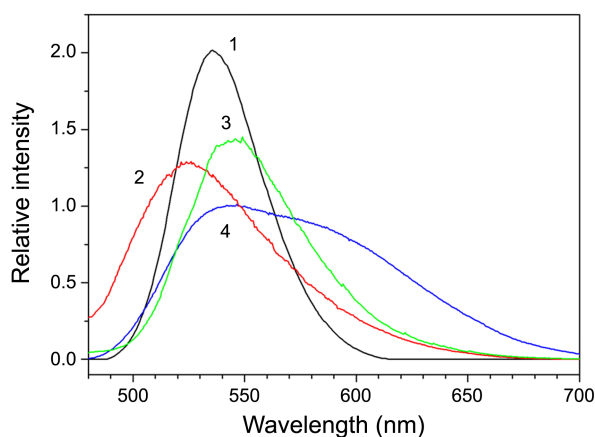


**Figure 8.** Luminescence ( $\lambda_{exn} = 460$  nm) spectra of  $(Zn_{0.6}Sr_{0.3}Mg_{0.1})_2Ga_2S_5:Eu^{2+}$  (1),  $CaBaSrSiO_4:Eu^{2+}$  (LWB, 2),  $\beta-SiAlON:Eu^{2+}$  (Denka, 3) and modified  $YAG:Ce^{3+}$  (Nemoto-432, 4) phosphors, and excitation spectrum of the green luminescence ( $\lambda_{ems} = 520$  nm).

green phosphor was stronger than that of the commercial yellow phosphor, the quantum yield of the green phosphor was lower than that of the modified  $YAG:Ce^{3+}$  phosphor ( $Q = 23.0\%$ ).<sup>16</sup> It could be due to the smaller bandwidth of the green phosphor. As shown in Figure 3, the excitation spectrum had its maximum intensity in the range 390-490 nm. This indicated that the blue GaN LED was suitable as a pumping source for the prepared green phosphor.

**Device Characterization.** MgO-coated green phosphor was casted on blue GaN LEDs with various weight percentages of the coated phosphor in epoxy. Figure 9 shows the luminescence spectrum of a fabricated pc-LED device. The spectrum consisted of two bands: a sharp band, peaking at 460 nm due to the emission from the pumping GaN diode, and a broad band, peaking at 532 nm due to the emission from the green phosphor. The CIE 1931 chromaticity of the pc-LEDs with different weight percentages of the green phosphor is shown in Figure 10. The chromaticity index (x, y) varied along the line from (0.1433, 0.0402) for the naked GaN chip to (0.3062, 0.6381) for the 10 wt % blended phosphor. Furthermore, the phosphor-cast white LEDs (pc-

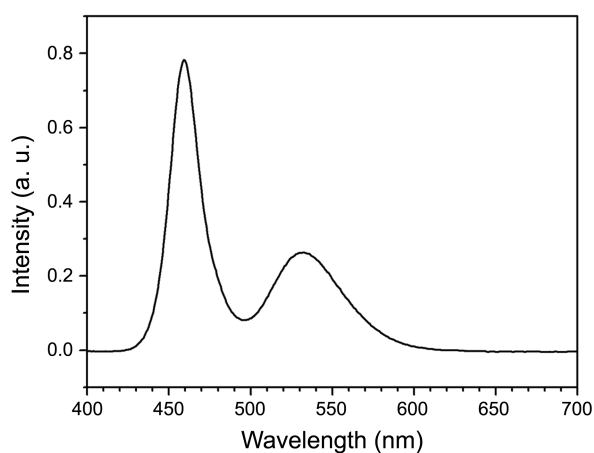


**Figure 9.** PL spectrum of phosphor-casted GaN LED (3 wt % phosphor casted).

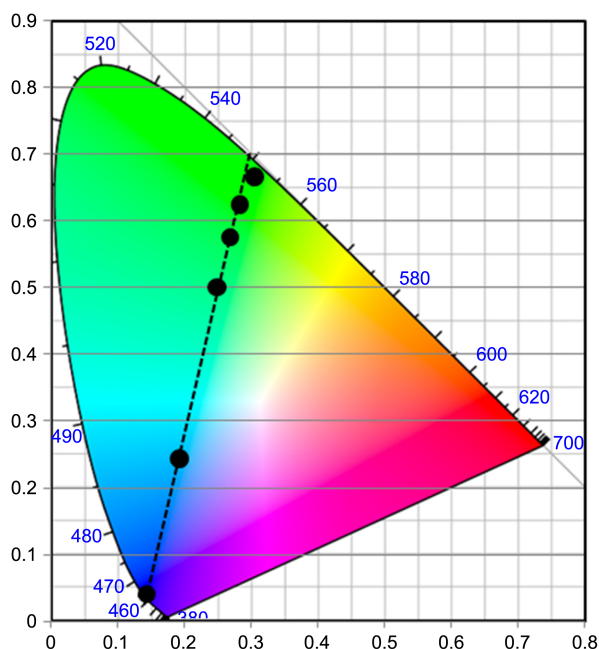


**Figure 10.** CIE indexes of GaN LED casted with various weight percentages of  $(\text{Zn}_{0.6}\text{Sr}_{0.3}\text{Mg}_{0.1})_2\text{Ga}_2\text{S}_5:\text{Eu}^{2+}$  (circles from lower to upper: 0, 1, 3, 5, 7 and 10 wt %).

WLEDs) using the optimized green (G) and the red  $(\text{Ca}_{0.85}\text{Sr}_{0.15})(\text{S}_{0.4}\text{Se}_{0.6}):\text{Eu}^{2+}, \text{Sc}^{3+}$  (R) phosphors,<sup>17</sup> and the commercial yellow (Y) phosphor was fabricated on blue GaN LEDs. The observed optical properties of the raw chip and the pc-WLEDs are listed in Table 1. The general color rendering index (CRI) and the corrected color temperature (CCT) of the two-band (B+Y) pc-WLED were 83 Ra and 6160 K, respectively. Specially, the two-band pc-WLED generated the overcast daylight. For the three-band pc-WLED, the relative luminance of the three-band (B+G+R) pc-WLED was slightly reduced. However, the CRI (86 Ra) and the CCT (5560 K) were improved, compared with the two-band pc-WLED. The three-band pc-WLED produced the noon daylight. These results suggested that the prepared phosphor might be a potential green phosphor for a prospective pc-WLED.

**Table 1.** Optical properties of the fabricated LEDs using the prepared green (G) and red (R), and the commercial yellow (Y) phosphors, and a blue LED chip

LED (wt %)	CIE (x, y)	CCT (K)	CRI (Ra)	Rel. Lum.
Blue chip	0.1479, 0.0543	-	-	1
Y (3)	0.3228, 0.3283	6160	83	5.2
G:R (1.1:1.9)	0.3313, 0.3289	5560	86	4.7

## Conclusions

Highly luminescent green phosphor with the chemical formula of  $(\text{Zn}_{1-a-b}\text{M}_a\text{M}'_b)_2\text{Ga}_2\text{S}_5:\text{Eu}^{2+}$  ( $\text{M}, \text{M}' =$  alkali earth ions) were prepared using non-toxic and inexpensive materials through a simple solid-state reaction. The partial replacements of  $\text{Zn}^{2+}$  by  $\text{Sr}^{2+}$  and  $\text{Mg}^{2+}$  ions enhanced the luminescence intensity more than 3-fold. Chemical stability of the prepared green phosphors was achieved using MgO thin-film coating on the surface of the phosphor. The phosphor-converted light-emitting diodes (pc-LEDs) were fabricated by casting the MgO-coated green phosphor with various weight percentages on GaN blue LEDs. The linearity of the chromaticity index of the pc-LED versus the wt % blended phosphor suggested that the color range of the light emitted by the pc-LED was easily adjustable as desired. The superior luminescence properties of the prepared green phosphor make it a good candidate for prospective solid-state lighting devices.

**Acknowledgments.** This study was financially supported by research fund of Chungnam National University in 2010.

## References

- Kim, J. W.; Kim, Y. J. *J. Nanosci. Nanotech.* **2007**, *7*, 4065.
- Kim, W.; Kim, Y. J. *J. Euro. Ceram. Soc.* **2007**, *27*, 3667.
- Wickleder, C.; Zhang, S.; Haeuselner, H. *Z. Kristallographie* **2005**, *220*, 277.
- Chartier, C.; Barthou, C.; Benalloul, P.; Frigerio, J. M. *J. Lumin.* **2005**, *111*, 147.
- Smet, P. F.; Moreels, I.; Hens, Z.; Poelman, D. *Mater.* **2010**, *3*, 2834.
- Huh, Y.-D.; Park, J.-Y.; Kweon, S.-S.; Kim, J.-H.; Kim, J.-G.; Do, Y. R. *Bull. Korean Chem. Soc.* **2004**, *25*, 1585.
- Nazarov, M.; Noh, D. Y.; Byeon, C. C.; Kim, H. *J. Appl. Phys.* **2009**, *105*, 073518.
- Inaho, S.; Hase, T. *Phosphor Handbook*; Shionoya, S., Yen, W. M., Eds.; CRC Press: New York, 1999; Ch. 4.
- Jung, H. S.; Lee, J.-K.; Nastasi, M.; Lee, S.-W.; Kim, J.-Y.; Park, J.-S.; Hong, K. S. *Langmuir* **2005**, *21*, 10332.
- (a) de Mello, J. C.; Wittmann, H. F.; Friend, R. H. *Adv. Mater.* **1997**, *9*, 230. (b) Kim, K.-B.; Kim, Y.-I.; Chun, H.-G.; Cho, T.-Y.; Jung, J.-S.; Kang, J.-G. *Chem. Mater.* **2002**, *14*, 5045.
- Chen, W.; Malm, J.-O.; Zwiller, V.; Huang, Y.; Liu, S.; Wallenberg, R.; Bovin, J.-O. *Phys. Rev. B* **2000**, *61*, 11021.
- Chen, W.; Malm, J.-O.; Zwiller, V.; Wallenberg, R.; Bovin, J.-O. *J. Appl. Phys.* **2001**, *89*, 2671.
- Tang, T. P.; Wang, W. L.; Wang, S. F. *J. Alloys Compd.* **2009**, *488*, 250.
- Li, G. H.; Su, F. H.; Ma, B. S.; Ding, K.; Xu, S. J.; Chen, W. *Phys. Stat. Sol. (b)* **2004**, *241*, 3248.

15. Park, S. H.; Park, J. K.; Kim, C. H.; Jang, H. G. *Bull. Korean Chem. Soc.* **2010**, *31*, 3075.  
16. Kang, J.-G.; Kim, M.-K.; Kim, K.-B. *Mater. Res. Bull.* **2008**, *43*,

1982.  
17. Shin, J.-S.; Kim, H.-J.; Jeong, Y.-K.; Kim, K.-B.; Kang, J.-G. *Mater. Chem. Phys.* **2011**, *126*, 591.

---